Instructions for Improving the Shape of Long-range Subsonic Airplanes and Gliders

IGOR NESTERUK
Institute of Hydromechanics
National Academy of Sciences of Ukraine
Kyiv
UKRAINE
ORCID: 0000-0001-7250-2729

Abstract: - Optimizing airplanes and gliders requires improving their shapes to reduce aerodynamic drag. In particular, the high weight-to-drag ratio (commercial efficiency) increases the range of the vehicles. Corresponding ideas and results are well-known. Nevertheless, high interest in unmanned vehicles requires simple instructions for engineers and managers. Analytic formulae for the drag-to-lift ratio of the optimal wing for the laminar and turbulent flow patterns are presented. The lift-to-drag ratio, angle of attack, and chord length of the optimal wings, drag on the optimal fuselage, commercial efficiency, engine power, and maximum range were estimated for subsonic airplanes and gliders with the given mass, cruise speed, wing aspect ratio, and fuselage volume. The wing aspect ratio must be as high as possible to achieve the maximum range. For certain combinations of the given parameters, the drag on the special-shaped, unseparated fuselages can be neglected in comparison to the drag on the optimal wing. The characteristics of the optimal aircraft with desirable values of range are estimated. The range of gliders can be comparable to the range of small electrical airplanes of the same commercial efficiency.

Key-Words: - unmanned vehicles, subsonic aircraft; gliders; range increase; commercial efficiency; unseparated shapes.

Received: March 9, 2026. Revised: April 11, 2026. Accepted: May 13, 2026. Published: July 16, 2026.

1 Introduction

The conceptual aircraft design allows initial estimating the characteristics of vehicles, such as drag, power, range, etc. [1], [2], [3], [4], [5]. The shape optimization includes low-fidelity approaches and corresponding software, which enables to improve the characteristics without using complicated and expensive CFD methods [2], [3], [4], [5]. The growing interest in drones requires the simplest possible recommendations for optimal wing and fuselage shapes in a wide range of vehicle masses and speeds.

The maximal commercial efficiency k (weight-to-drag ratio) ensures the maximum range of vehicles that have a fixed amount of fuel (or another energy) on board [1, 6-8]. The range of a glider descending in calm air is also proportional to the value of k [8]. When the mass of a vehicle m is fixed, its maximum range corresponds to the minimum drag X, which can be approximately divided into two parts $X = X_W + X_U$. For the steady horizontal motion, the drag on the wing X_W is practically independent of the cruise speed U and the drag on the fuselage X_U increases with speed. Both main components of the drag were estimated for the optimal wing (with the lowest drag – the sum of the friction and inductive resistance) and for the body of revolution without boundary-layer separation [7, 8]. The examples of calculations presented in [8] yield very high values of the wing aspect ratio $\lambda = b/H$ (b is span, H is the average chord length), which are possible for record gliders (see, e.g., [9, 10]). However, considerations of strength and cheapness of aircraft construction can severely limit the allowable values of the wing aspect ratio.

In this paper, we propose an algorithm of seeking the optimal wing with the given values of λ, the vehicle mass, and cruise speed. The critical velocities, when the drag on the fuselage can be neglected, will be calculated. The total drag, the cruise, and available powers [11] will be estimated and compared with the average characteristics of aircraft presented in [11]. The inverse problem of finding the optimal wing aspect ratio, its chord and angle of attack will be solved for given values of the range.

2 Materials and Methods

We will use the estimations for the laminar and turbulent flow of incompressible fluid [7], [8]. It means that only subsonic vehicles will be considered with the cruise speed U<150 m/s. Then the lift-to-drag ratio

$$k_W = \frac{Y}{X_w} = \frac{mg}{X_w} \tag{1}$$

of the optimal wing can be calculated as follows [7]:

$$k_{W,lam} \approx 0.54\lambda^{1/2}\,\mathrm{Re}_H^{1/4},$$
$$k_{W,tur} \approx 3.58\lambda^{1/2}\,\mathrm{Re}_H^{1/14} \tag{2}$$

$$\mathrm{Re}_H = \frac{UH}{\nu} \tag{3}$$

where Re_H is the Reynolds number based on the average chord length H=S/b (S and b are the area and the span of a wing); ν is the kinematic viscosity of air. Estimations (2) are valid for the slender wings (their maximal thickness has to be much smaller than H).

The optimal value of the lift force $Y_{opt} = k_W X$, corresponding to the maximum efficiency, can be estimated as follows, [8]:

$$Y_{opt,lam} \approx 1.43\lambda^{3/2}\,\mathrm{Re}_H^{7/4}\rho\nu^2 ,$$
$$Y_{opt,tur} \approx 0.22\lambda^{3/2}\,\mathrm{Re}_H^{27/14}\rho\nu^2 \tag{4}$$

for the laminar and turbulent flows. The corresponding optimal angles of attack α_{opt}, [8]:

$$\alpha_{opt,\,lam} \approx 0.46\lambda^{1/2}\,\mathrm{Re}_H^{-1/4} \quad , \qquad \alpha_{opt,\,tur} \approx 0.07\lambda^{1/2}\,\mathrm{Re}_H^{-1/14} \tag{5}$$

were estimated with the use of the known linear dependence for the lift coefficient $C_y \equiv 2Y/(\rho U^2\lambda_W H^2) = 2\pi\alpha$ for a slender symmetric airfoil (see, e.g., [12]); ρ is the density of air.

For given values of the mass of a vehicle (its weight mg is equal to the lift force Y_{opt} in a horizontal cruise flight) and the aspect ratio of its wing, eq. (4) allows us to determine the corresponding Reynolds numbers of the optimal wing:

$$\mathrm{Re}_{H,lam} = \left[\frac{mg}{1.43\lambda^{3/2}\rho\nu^2}\right]^{4/7} \tag{6}$$

$$\mathrm{Re}_{H,tur} = \left[\frac{mg}{0.22\lambda^{3/2}\rho\nu^2}\right]^{14/27} \tag{7}$$

for the fully laminar and the fully turbulent flows, respectively. Since the flow can remain laminar for any disturbances at Re_H <60,000 (see e.g., [7]), we will use formula (6) at $\mathrm{Re}_H < 10^5$ and (7) at $\mathrm{Re}_H \ge 10^5$. The use of special shaped wings allows obtaining laminar flow at much higher Reynolds numbers (see, e.g., [9, 10]). In this case, the critical Re_H value can be higher, but eqs. (6) and (7) are still valid. Formulae (2), (6) and (7) allow us to obtain relationships for the lift-to-drag ratio of the optimal wing in the laminar and turbulent case, respectively:

$$k_{W,lam} \approx 0.51\lambda^{2/7}(mg)^{1/7}\rho^{-1/7}\nu^{-2/7},$$
$$k_{W,tur} \approx 3.79\lambda^{4/9}(mg)^{1/27}\rho^{-1/27}\nu^{-2/27} \tag{8}$$

which demonstrate the increase with the weight of the vehicle and the wing aspect ratio. From (5)-(7), the following formulae for the angle of attack of the optimal wing in the laminar and turbulent case can be obtained:

$$\alpha_{opt,lam} \approx 0.48\lambda^{5/7}(mg)^{-1/7}\rho^{1/7}\nu^{2/7},$$
$$\alpha_{opt,tur} \approx 0.066\lambda^{5/9}(mg)^{-1/27}\rho^{1/27}\nu^{2/27} \tag{9}$$

which demonstrate the decrease with the weight of the vehicle and increase with the wing aspect ratio. Multiplying (6) and (7) by corresponding values of the kinematic velocity (according to eq. (3)) yields the optimal values of UH at different heights of the cruise flight. All these characteristics and the drag on the optimal wing are independent of the cruise speed. In particular, it follows from (1) that

$$X_w = \frac{mg}{k_W} \quad (10)$$

The average chord length is inversely proportional to the speed and can be obtained from (6) and (7):

$$H_{lam} \approx 0.82 U^{-1} \lambda^{-6/7} (mg)^{4/7} \rho^{-4/7} \nu^{-1/7},$$
$$H_{tur} \approx 2.19 U^{-1} \lambda^{-7/9} (mg)^{14/27} \rho^{-14/27} \nu^{-1/27} \quad (11)$$

for the laminar and turbulent cases, respectively.

The drag on the fuselage depends on the speed and its volume V, and can be reduced with the use of special-shaped bodies of revolution, which ensure the flow pattern without boundary-layer separation [7], [13], [14]. For the laminar flow, the volumetric drag coefficient

$$C_V = \frac{2X_U}{\rho U^2 V^{2/3}} \quad (12)$$

was estimated as follows, [7]:

$$C_V = \frac{4.7}{\sqrt{\mathrm{Re}_V}}, \qquad \mathrm{Re}_V = \frac{UV^{1/3}}{\nu} \quad (13)$$

According to (13), the volumetric drag coefficient is independent of shape, decreases with an increase in the volumetric Reynolds number Re_V, and attains a minimum at the critical value of the Reynolds number, corresponding to the following relationship [8, 15]:

$$\frac{UV}{L^2} = 1.81 \cdot 10^5 \nu \quad (14)$$

where L is the fuselage length. For very slender, special-shaped bodies of revolution (D/L<0.05, D is the maximum diameter) C_V could be smaller than 0.001 at Reynolds numbers close to the critical one. At greater values of Re_V, the turbulence rapidly increases the volumetric drag coefficient, which is practically independent of the thickness ratio D/L and approaches the value

$$C_V \approx 0.01, \quad (15)$$

(see [7]). Since there is no dependence on the body shape in eqs. (13) and (15), any unseparated shape proposed in [7], [13], [14] can be used for a low-drag fuselage.

According to (12)-(15), the drag on such a fuselage can be presented as follows:

$$X_U = 0.5 C_V \rho U^2 V^{2/3} = \begin{cases} 2.35 \rho \sqrt{\nu V U^3}, & U \le 1.81 \cdot 10^5 \nu L^2 / V \\ 0.005 \rho U^2 V^{2/3}, & 1.81 \cdot 10^5 \nu L^2 / V < U < 150 m/c \end{cases} \quad (16)$$

At small speeds, the drag on the special-shaped fuselages can be neglected [7], [8]. To calculate the corresponding critical values of speed U^*, let us use the condition:

$$X_U = \frac{X_w}{10} = \frac{mg}{10 k_W} \quad (17)$$

Then it follows from (16) and (17) that

$$U^* = \begin{cases} 0.122 \sqrt[3]{\dfrac{m^2 g^2}{k_W^2 \rho^2 \nu V}}, & U^* \le 1.81 \cdot 10^5 \nu L^2 / V \\ \dfrac{4.47}{\sqrt[3]{V}} \sqrt{\dfrac{mg}{k_w \rho}}, & 1.81 \cdot 10^5 \nu L^2 / V < U^* < 150\, m/s \end{cases} \quad (18)$$

At speeds smaller than U^*, the drag on special-shaped unseparated fuselages can be neglected in comparison with the drag on the wing. The critical velocity depends both on the vehicle mass and the volume of the fuselage (see (18)). Since these values are related, let us use approximate average relationships for the typical propeller and turboprop aircraft, obtained in [11] after averaging statistical information:

$$D \approx 0.0481 (mg)^{1/3}, \qquad L \approx 0.41 (mg)^{1/3} \quad (19)$$

(m is in kilograms, the fuselage length and diameter are in meters). Taking into account the empirical formula for the volume of typical fuselages, [16]:

$$V \approx 0.6\pi(D/2)^2 L, \quad L \approx 0.47 D^2 L \tag{20}$$

and (19), the relationship (18) can be rewritten as follows:

$$U^* = \begin{cases} 1.6\sqrt[3]{\dfrac{mg}{k_W^2 \rho^2 \nu}}, & U^* \le \dfrac{6.82 \cdot 10^7 \nu}{\sqrt[3]{mg}} \\ \dfrac{58.5(mg)^{1/6}}{(k_w \rho)^{1/2}}, & \dfrac{6.82 \cdot 10^7 \nu}{\sqrt[3]{mg}} < U^* < 150\, m/s \end{cases} \tag{21}$$

The accuracy of formula (21) is limited due to the limited accuracy of eqs. (19) and (20) even for standard fuselages. Especially large discrepancy is expected for special shaped unseparated fuselages [7], [13], [14]. For such fuselages direct estimations of their drag and comparison with the drag on the wing can be recommended.

Let us estimate the fuselage wetted area of the typical aircraft with the use of (20) and the Hoerner empirical formula (see [16]) $S_f \approx 0.7\pi DL$. Then

$$S_f \approx 0.7\pi DL \approx 0.043(mg)^{2/3} \tag{22}$$

Supposing that the drag on the typical fuselage is proportional to its wetted area and the drag on the optimal wing is twice as larger as the friction drag (see, e.g., [12]), which is proportional to the wetted area of the slender wing $S_{fW} \approx 2S$. Finally, with the use of dependence of the wing area of a typical aircraft [11]:

$$S \approx 0.0262(mg)^{2/3}$$

we obtain

$$\frac{X_w}{X_U} \approx 2.44 \tag{23}$$

The ratio (23) is independent of the speed and demonstrates that for the typical aircraft, the drag on the wing is significantly larger than the drag on the fuselage. Eq. (21) will allow us to find the velocity ranges when the drag on the fuselage can be neglected.

When the drag on the fuselage can be neglected, the commercial efficiency is close to the lift-to-drag ratio of the wing:

$$k = \frac{mg}{X} \approx \frac{mg}{X_U + X_w} \approx \frac{mg}{X_w} = k_W \tag{24}$$

In particular, the commercial efficiency of the ETA glider [9] is very close to the second estimation (8).
The cruising power

$$N = UX \approx UX_w = \frac{mgU}{k} \tag{25}$$

corresponds to the mechanical power of the steady motion when the thrust is equal to the drag. Values of N are much lower than the real power of engines N_A (the available power) since only a part of the available energy can be transformed into the energy of motion [7], [8], [11]. To estimate the differences between N and N_A, the corresponding results of statistical averaging can be used [11]:

$$N \approx 1.67(mg)^{7/6} \tag{26}$$

$$N_A \approx 5.25(mg)^{1.13} \tag{27}$$

(the powers are in watts, mass is in kilograms). It follows from (26) and (27) that

$$p_1 = \frac{N_A}{N} \approx \frac{3.14}{(mg)^{0.037}} \tag{28}$$

The value of parameter p_1 diminishes with the increase of the vehicle weight and varies from 3.7 to 2 for the mass range 0.01kg - 300 t. From (25) and (28) we can obtain

$$N_A \approx \frac{p_1 mgU}{k} \tag{29}$$

Eq. (29) demonstrates that at fixed mass and available power, aircraft with maximal commercial efficiency k have the maximal speed.

With a given energy reserve on board Q, which is used evenly over time T, the range R can be estimated as follows:

$$R = UT = \frac{UQ}{N_A} \approx \frac{kQ}{p_1 mg}$$
(30)

With the use of energy reserve per unit weight q and taking into account that the fuel tanks (batteries) make up only a portion of the aircraft weight $p_2 mg$; $p_2 < 1$, eq. (30) can be rewritten as follows:

$$R \approx \frac{kp_2 q}{p_1}$$
(31)

When the drag on the fuselage can be neglected, the commercial efficiency k can be replaced by k_W in (31). In particular, for an electrical aircraft with batteries providing an energy reserve of approximately 1000kJ per kilogram of weight [17] q=10^5 J/N =10^5 m =100 km. Then eq. (31) yields:

$$R_e \approx \frac{100kp_2}{p_1} \quad (km)$$
(32)

For the gasoline engines the corresponding range will be approximately 9-19 times higher (due to the much higher specific energy - 46.4 MJ per kilogram of petrol weight [18], 20%-40% of which can be converted into mechanical energy [19]), the corresponding range will be approximately 9-19 times higher. For gliders descending in the calm atmosphere from the height h the values q=h; $p_1 = p_2 = 1$. Then eq. (31) yields (see also [8])

$$R_g \approx kh$$
(33)

3 Results and Discussion

Figs. 1-4 represent the results of calculations with the use of formulae (6)-(9), (21) for different values of the wing aspect ratio (corresponding curves have different colors shown in Figure 1). Two heights of a cruise flight: around 0 km (solid curves) and 10 km (dotted lines) with the values of the air density and viscosity corresponding to the standard atmosphere [20] were used. To avoid separation, the angle of attack has to be limited. For the case of the thin symmetrical airfoil under consideration, we have taken the value of 10 degrees as the maximum permissible angle of attack and have shown only the values corresponding to smaller angles of attack. At m<100kg, jumps in the values are associated with the laminar-to-turbulent transition on the wing (at $\mathrm{Re}_H = 10^5$).

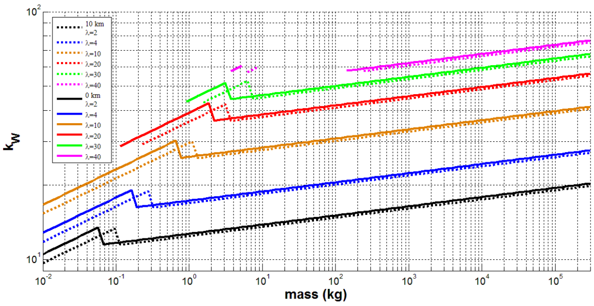

Fig. 1: The lift-to-drag ratio of the optimal wing versus the vehicle mass at different wing aspect ratios and the height of the cruise flight. Solid lines correspond to the flight near the surface, dotted ones – the height 10 km

High values of the lift-to-drag ratio k_W correspond to the low drag on the wing (see (10)) and the large range of vehicles. Figure 1 illustrates the increase in k_W for high values of the wing aspect ratio $\lambda = b/H$. If considerations of the structural strength of a vehicle limit the value of , its economic efficiency decreases. Values of k_W are also limited by the angles of attack of the optimal wing (calculated with the use of (9) and shown in Figure 2). In particular, for small vehicles (m <0.1kg) k_W<25, if the angle of attack cannot exceed 10º (see Figure 1 and Figure 2).

Figs. 1-3 allow designers of a new vehicle to preliminarily assess its commercial efficiency, angle of attack, and the chord length for different values of the wing aspect ratio. The aspect ratio of the typical aircraft wing is 8.15, [11]. To have higher commercial efficiency, values have to be increased as much as possible. For example, ETA glider [9, 10] with =51.33 has achieved the value of k=70. After the proper value of is selected, the maximal value of the lift-to-drag ratio and the angle of attack can be calculated with the use of (8) and (9) for any height of cruise flight for a vehicle of given mass. Then the drag on the wing can be assessed using eq. (10). At a given speed of the cruise flight, the average chord length can be estimated from Figure 3. The exact values of H and the wing span $b = \lambda H$ can be found with the use of (11).

The wing span of the long-range aircraft can be rather large (since it increases with the increase in , see (11)). This may impose additional restrictions on applications of the vehicle, raising questions about the possibility of using two or more wings. Neglecting the interference between two equal wings, the commercial efficiency of the 2-wing concept can be estimated using eqs. (8) and (10). Putting mg/2 into (8), we obtain $2^{1/7} \approx 1.10$ and $2^{1/27} \approx 1.03$ times lower values of k_W for the laminar and turbulent cases, respectively. Accordingly, the total drag on two wings will be 10% and 3% higher than on one wing with the same aspect ratio supporting the total weight. The 2-wing concept can be preferable for small aircrafts, when one turbulent wing can be replaced by two laminar ones. E.g., with m=2 kg, =10 and the height of the cruise flight 10 km (ρ=0.414 kg/m^3, ν=3.525*10^{-5} m^2/s, [20]) the second formula (8) yield $k_{W,tur} \approx 26$ (see the brown dotted curve in Figure 1). A laminar wing with =10 supporting the half-weight 1 kg enables to have $k_{W,lam} \approx 29$ (see the first formula (8) and the brown dotted curve in Figure 1). Thus, the drag on two laminar wings could be 12% lower provided the interference is neglected. The interference depends on the aircraft design and can be taken into account with the use of CFD methods or experiments.

Fig. 2 demonstrates that the optimal angle of attack of very small vehicles increases drastically even for small values of λ. E.g., taking the characteristics of the bee ($\lambda \approx 7$, $m \approx 100mg$, [7]) flying near the earth's surface, we can obtain $\alpha_{opt,lam} \approx 17.6^o$ using the first formula (9). At such high values of the angle of attack, it is impossible to avoid separation. Maybe it is the reason why bee and other insects use very specific unsteady flow patterns with the very high frequency of wing oscillations, [21].

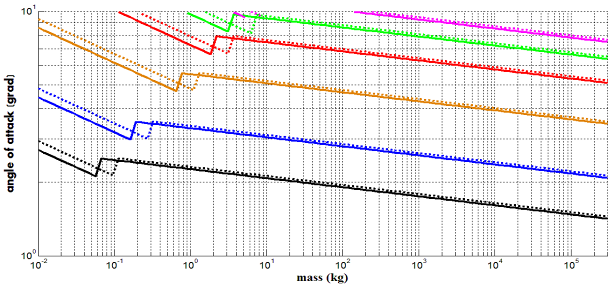

Fig. 2: The angle of a ttack of the optimal wing using a slender symmetric airfoil versus the vehicle mass at different wing aspect ratios and the height of the cruise flight. Solid lines correspond to the flight near the surface, dotted ones – the height 10 km. Different colors of curves correspond to different wing aspect ratios shown in Fig.1

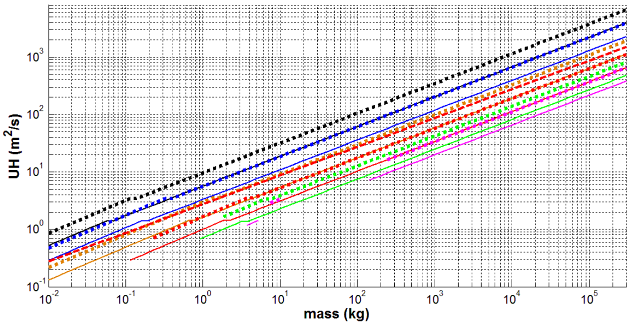

Fig. 3: The UH values for the optimal wing versus the vehicle mass at different wing aspect ratios and the height of the cruise flight. Solid lines correspond to the flight near the surface, dotted ones – the height 10 km. Different colors of curves correspond to different wing aspect ratios shown in Fig.1

Drag on the fuselage decreases with the decrease of its volume and the speed of the cruise flight. It can be estimated using (16) if special-shaped unseparated bodies of revolution (proposed in [7], [13], [14] or other shapes, which can be calculated to order) are used. If it is possible, their volume, length, and speed have to be related according to (14) in order to achieve the laminar flow pattern and the minimal drag on the fuselage. Then, at high velocities, the values V/L^2 have to be small and the elongation (L/D ratio) of the laminar hulls increases with the increase of the velocity. As in the case of the wing, L/D values are limited by the structural strength of a vehicle. When the condition (14) does not hold, the boundary-layer on the same shapes become turbulent and the drag increases (see eq. (16) and corresponding jumps in U* values at m >300 kg in Figure 4).

The fuselage shape of the ETA glider [9, 10] is similar to ones presented in [14] and probably ensures the laminar flow pattern with $UV < 1.81 \cdot 10^5 \nu L^2$ (see estimations in [8]). The U* values, corresponding to the mass of this glider (850 kg), are higher than 30 m/s (see Figure 3). It means that the drag on its fuselage can be neglected in comparison with the drag on its wing at U<30 m/s. Figure 4 demonstrates that the drag on the unseparated fuselage can be neglected at U<30 m/s and m>200kg. Probably, at small enough speeds even not so good-shaped fuselages can ensure much lower drag than the drag on the wing (e.g., Solar Impulse 2 plane with U=17 m/s and m=2300 kg, [22]).

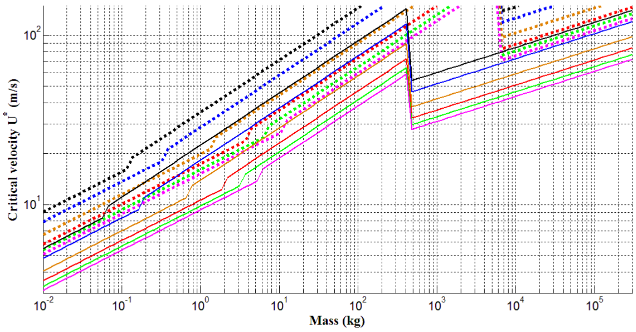

Fig. 4: The critical velocity versus the vehicle mass at different wing aspect ratios and the height of the cruise flight. Solid lines correspond to the flight near the surface, dotted ones –the height 10 km. Different colors of curves correspond to different wing aspect ratios shown in Fig.1

Generally (when the drag X_U on the fuselage is significant), the total drag can be calculated with the use of (16) and (24). Then the commercial efficiency k, the power P_A, and the range can be estimated with the use of (24), (29), and (31), respectively. On the other hand, fixing the desirable range of the vehicle, corresponding values of k can be estimated from (31)-(33). Assuming that $k \approx k_w$, corresponding values of the wing aspect ratio can be estimated from Figure 1 or eq. (8).

For example, let us find the characteristics of an electrical aircraft with a range of 1000 km. According to (32), the commercial efficiency of such a vehicle has to be:

$$k \approx \frac{10 p_1}{p_2}$$
(34)

Taking into account that $2 \le p_1 \le 3.7$ (according to (28)) and putting, e.g., p_2=0.5 (the weight of the accumulators is a half of the total vehicle weight), eq. (34) yields $40 \le k \le 74$. Fig.1 illustrates that for the large aircrafts (the lower limit of k), the desirable range is possible even at moderate values of the wing aspect ratio $\lambda \approx 10$. Small aircrafts (the higher limit of k) cannot have a range of 1000 km. High values of U* (see Figure 4) show that the drag on special-shaped unseparated fuselages can be neglected, i.e., $k \approx k_w$ for the large aircrafts. For some medium aircraft mass (e.g., 300 kg) $p_1 \approx 2.34$; $k \approx 46.8$ (according to (28) and (34)), the desirable range is possible, but with rather high wing aspect ratios ($\lambda > 30$, see Figure 1).

The range 500 km is achievable for the medium electrical aircraft of mass 300 kg at rather small values of λ, since $k \approx 23.4$ (see eq. (28) and Figures 1, 4). If m=10 kg, the values $p_1 \approx 2.65$; $k \approx 26.5$ and Figure 1 demonstrate that the aspect ratio of the optimal wing must be around 10. The corresponding values of critical velocity are lower than 30 m/s. It means that for fast vehicles with U> U* we can use the condition $k \approx k_w$ and formulae (8) only for preliminary estimations of λ values. With the given speed and volume of a special-shaped fuselage, the drag X_U can be calculated, and the corrected value of k can be found from eqs. (10) and (24). The procedure should be repeated until convergence. In any case, the λ values will be larger than 10 for the optimal electrical aircraft of mass 10 kg and range 500 km.

As mentioned in the previous Section, the use of gasoline engines allows increasing the range 9-19 times with the same values of commercial efficiency and parameters p_1 and p_2. In particular, we can have the mentioned before ranges with 9-19 times smaller values of parameter p_2 (there is no need to use the half of the vehicle weight for fuel). On the other hand, the vehicles with estimated before optimal characteristics and p_2=0.5 can have 9-19 times higher range. E.g., at m=300 kg and p_2=0.5 the range 4,500-9,500 km is achievable using the wing with λ= 4.9-5.1 (obtained from the second formula (8) for $k = k_W = 23.4$ and different heights of the cruise flight). Since the critical velocity U^* is rather high (see Figure 4), the use of special-shaped laminar fuselages will allow neglecting their drag even at speeds around 100 m/s. The corresponding angles of attack and the average chord length can be found from (9) and (11).

It must be noted that the ranges of small electrical aircrafts and gliders can be rather close at large enough values of the initial glider height h. In particular, they are equal at some critical value

$$h^* \approx \frac{100 p_2}{p_1} \quad (km)$$
(35)

following from (32) and (33). Putting p_1=3.7 and p_2=0.5 into formula (35), we can conclude that the glider descending from the height more than 13.5 km has a larger range than a small electrical airplane of the same commercial efficiency.

4 Conclusions

Simple formulae and diagrams are proposed in order to assess the lift-to-drag ratio, the angle of attack, and the chord length of the optimal wings, drag on the optimal fuselage, the commercial efficiency, the engine power, and the maximal range of subsonic airplanes and gliders. The total drag, the cruise, and available powers were estimated with the use of the approach developed before by the author and the average characteristics of aircraft presented in [11]. The proposed formulae and diagrams allowed solving the inverse problem of finding the optimal wing aspect ratio, its chord and angle of attack for given values of the range.

The shape of optimal vehicles and their characteristics were calculated for the given mass, cruise speed, wing aspect ratio, and fuselage volume. To achieve a desirable range, the same formulae can be used to estimate the optimal values of the wing aspect ratio, chord, angle of attack and span. The proposed simple approach could be useful for engineers and managers developing new vehicles.

It was shown that the wing aspect ratio must be as high as possible to achieve the maximum range. For some combinations of the given parameters, the drag on the special-shaped unseparated fuselages can be neglected in comparison with the drag on the optimal wing. The corresponding formula for the critical speed is presented. It was shown that the range of gliders can be comparable to the range of small electrical airplanes of the same commercial efficiency.

References:

[1] Raymer, D.: Aircraft Design: A Conceptual Approach, Sixth Edition. ISBN: 978-1-62410-490-9 (2018). DOI: 10.2514/4.104909
[2] Ünal, N., Öz, Y., Oktay, T.: Conceptual design modeling by the novel aircraft conceptual design and analysis system (ACDAS). Aircraft Engineering and Aerospace Technology: An International Journal. 95 (5), 799–813 (2023). doi: https://doi.org/10.1108/AEAT-02-2022-0056
[3] Ullah, A: Optimizing UAV Wing Performance: A Computational Analysis with Computer-Based Algorithms for Composite Material Integration. International Journal of Innovations in Science & Technology, 50sea, vol. 6(1), 287-300 (2024). https://ideas.repec.org/a/abq/ijist1/v6y2024i1p287-300.html
[4] Tarikul Islam, S.M., Xu, Y., Zaw, N.C.: Low-Fidelity Rapid Wing Design Optimization Approach for UAV. In: Zhu, Z.H.(., Wei, X., Li, R. (eds) Trends in Advanced Unmanned Aerial Systems. ICAUAS 2024. Springer Aerospace Technology. Springer, Singapore (2025). https://doi.org/10.1007/978-981-96-3240-4_23
[5] Vegh, J.M., Basset, PM., Beals, N. et al.: A comparison of three conceptual design approaches applied to an electric distributed lift aircraft. CEAS Aeronaut J . 16, 1227–1241 (2025). https://doi.org/10.1007/s13272-024-00766-2
[6] Gabrielly, Y., von Karman, Th.: What price speed. Mechanical Engineering, USA. 72(10), 775-779 (1950).
[7] Nesteruk, I.: Efficiency of Steady Motion and its Improvement with the Use of Unseparated and Supercavitating Flow Patterns. KPI Science News 6, 51-67 (2016). https://doi.org/10.20535/1810-0546.2016.6.81605.
[8] Nesteruk, I. Shape optimization principles for long-range unmanned vehicles. KPI Science News, no. 1–4, pp. 49–61 (2024). doi: 10.20535/kpisn.2024.1-4.314223 (in Ukrainian). https://concordia-sailplane.com/design-of-a-competition-sailplane/
[9] Dillinger, J., Boermans, L.M.M.: Aerodynamic Design of the Open Class Sailplane Concordia. XXVIII OSTIV Congress, Eskilstuna, Sweden, June 2006.
[10] Tianshu Liu: Comparative Scaling of Flapping and Fixed Wing Flyers. AIAA Journal, 44 (1) (2006).
[11] Loitsyanskiy, L.G.: Mechanics of Liquids and Gases. Begell House, New York and Wallingford, 6th ed. (1995).
[12] Nesteruk, I.: Rigid Bodies without Boundary-Layer Separation. Int. J. of Fluid Mechanics Research. 41(3), 260-281 (2014).
[13] Nesteruk, I.: Maximal speed of underwater locomotion. Innov Biosyst Bioeng 3(3), 152-167 (2019). https://doi.org/10.20535/ibb.2019.3.3.177976
[14] Nesteruk, I.: Low-Drag Bodies of Revolution and Their Applications for Effective Transportation.Transportation

Development Research. 3(2): 1–8 (2025). DOI: https://doi.org/10.55121/tdr.v3i2.697
[15] Hoerner, S. F.: Fluid-dynamic drag, Midland Park, N.J (1965).
[16] Weir, R. D., Nelson, C. W.: Utilization of poly(ethylene terephthalate) plastic and composition-modified barium titanate powders in a matrix that allows polarization and the use of integrated-circuit technologies for the production of lightweight ultrahigh electrical energy storage units (EESU). US patent 7466536, published 16 December 2008
[17] IOR Energy. List of common conversion factors (Engineering conversion factors)
[18] Daniel Barba, D.: ASSESSING THE EFFICIENCY POTENTIAL OF FUTURE GASOLINE ENGINES. (PDF). epa.gov. United States Environmental Protection Agency. (2018)
https://www.engineeringtoolbox.com/international-standard-atmosphere-d_985.html
https://www.sciencedaily.com/releases/2009/05/090507194511.htm
https://aroundtheworld.solarimpulse.com/adventure

Contribution of Individual Authors to the Creation of a Scientific Article (Ghostwriting Policy)

The author contributed in the present research, at all stages from the formulation of the problem to the final findings and solution.

Sources of Funding for Research Presented in a Scientific Article or Scientific Article Itself

No funding was received for conducting this study.

Conflict of Interest

The author has no conflicts of interest to declare that are relevant to the content of this article.